Boosted Kerr black holes in general relativity

Ivano Damião Soares[*]
Centro Brasileiro de Pesquisas Físicas—CBPF/MCTI, Rua Dr. Xavier Sigaud 150, Urca, CEP 22290-180 Rio de Janeiro, Brazil

(Received 15 October 2018; published 30 April 2019)

A solution of Einstein's vacuum field equation is derived that describes a general boosted Kerr black hole relative to a Lorentz frame at future null infinity. The metric contains five independent parameters—mass m, rotation ω, boost parameter v/c and the boost direction defined by (n_1, n_2, n_3) satisfying $(n_1)^2 + (n_2)^2 + (n_3)^2 = 1$—and reduces to the Kerr black hole when the boost parameter is zero and $n_1 = 1$. The solution describes the most general configuration that an astrophysical black hole must have. The black hole rotates about the z axis with angular momentum proportional to $m\omega$ and the geometry has just one Killing vector $\partial/\partial u$, where u is the retarded time coordinate. The boost turns the ergosphere asymmetric, with dominant lobes in the direction opposite to the boost. The event and Cauchy horizons, defined for the case $\omega < m$, are specified respectively by the radii $r_{\pm} = m \pm \sqrt{m^2 - \omega^2}$. The horizons are topologically spherical and the singularity has the topology of a circle on planes that are orthogonal to the boost direction. We argue that this black hole geometry is the natural set to describe the remnants of the recently observed gravitational wave events GW150914, GW151226, GW170814 and GW170817 [B. P. Abbott *et al.* (LIGO and Virgo Collaborations), Phys. Rev. Lett. **116**, 061102 (2016); **116**, 241103 (2016); **119**, 141101 (2017); **118**, 221101 (2017)]. In the conclusions we discuss possible astrophysical processes in the asymmetric ergosphere and the electromagnetic dynamical effects that may result from the rotating black hole moving at relativistic speeds.

DOI: 10.1103/PhysRevD.99.084054

I. INTRODUCTION

The Kerr black hole [1] is an exact stationary solution of vacuum Einstein equations of general relativity that describes a rotating black hole with two parameters, mass and angular momentum, and has the Schwarzschild black hole [2] as its static configuration limit. The Kerr solution turned out to be of fundamental importance to the understanding of astrophysical processes involved in objects with a tremendous output of energy as quasars, pulsars and active galactic nuclei (AGN). The recent direct observations of the gravitational wave emission from binary black hole mergers—GW150914 [3], GW151226 [4], GW170814 [5], GW170817 [6]—by the LIGO Scientific Collaboration and the Virgo Collaboration showed that the initial black holes of each binary had mass ratios $\alpha_{GW150914} \simeq 0.8$, $\alpha_{GW151226} \simeq 0.53$, $\alpha_{GW170104} \simeq 0.62$ and $\alpha_{GW170914} \simeq 0.83$, respectively. The nonequal mass of the initial black holes in the observed binaries imply that the gravitational waves emitted have a nonzero gravitational wave momentum flux, indicating that the remnant black hole is a Kerr black hole boosted along a particular direction relative to the asymptotic Lorentz frame at null infinity where such emissions have been detected. In this sense the remnant black hole description must contain additional parameters—the boost parameters—connected to its motion relative to the observation frame. The boost of the remnant black hole results from the net momentum flux of the gravitational waves emitted in the collision and merger of two nonequal mass black holes that generated the remnant.

The main object of this paper is to describe an exact solution of a general boosted Kerr black hole relative to an asymptotic Lorentz frame at future null infinity. This solution corresponds to the most general configuration that an astrophysical remnant black hole must have, in particular as the remnant configuration of the collision and merger of black holes recently observed in the direct detection of gravitational waves [3–6]. The derivation and interpretation of this solution will be framed in the Bondi-Sachs (BS) characteristic formulation of gravitational wave emission in general relativity [7–10], where we have a clear and complete derivation of physical quantities and its conservation laws, connected to the radiative wave transfer of energy and momentum, namely, the mass and momentum extracted of the system by the gravitational waves emitted, evaluated at future null infinity ($r \to \infty$), where the spacetime is asymptotically flat. In the BS formulation the conservation laws and final values of the conserved quantities are exact. The formulation [7,8] relies

[*]ivano@cbpf.br

on (i) expanding the metric functions in a power series of $1/r$ (where r is the luminosity distance), (ii) taking into account the BS boundary conditions (connected to the asymptotic flatness of the spacetime and the outgoing wave condition), (iii) using Einstein's vacuum equations and (iv) eliminating some arbitrary functions that arise in the integration scheme. This procedure is far from being trivial, and furthermore the coordinate system used may present singularities for r sufficiently small [7–10]. In this sense the use of the above procedures to obtain the exact metric of the remnant spacetime, expected to be that of a general boosted Kerr black hole, remains to be done. An analogous difficulty occurs in the case of $1+3$ numerical relativity simulations.

To circumvent this problem we will undertake the integration of Einstein's equation for stationary twisting Petrov D vacuum spacetimes, as discussed in the present paper. Among this Petrov type D class we will obtain a spacetime solution that corresponds to a Kerr black hole with additional parameters connected to the motion of the black hole relative to an asymptotic Lorentz frame at future null infinity; as the boost parameters go to zero we recover the Kerr metric [1]. This metric is therefore a candidate to describe an astrophysical remnant black hole, in particular the remnant configuration of the collision and merger of black holes recently observed in the direct detection of gravitational waves [3–6]. We also discuss that the boosted black hole solution can be a natural set for astrophysical processes connected to the asymmetry of the ergosphere and to electromagnetic dynamical effects that result from the rotating black hole moving at relativistic speeds in a direction not coinciding with the rotation axis of the black hole. These effects may correspond to the electromagnetic counterpart of the gravitational wave emission by the black hole having possibly the same order of magnitude. The paper extends our previous result obtained in the axisymmetric case [11].

Throughout the paper geometric units $G=c=1$ are used.

II. DERIVATION OF THE SOLUTIONS

In obtaining the metric of a stationary nonaxisymmetric boosted Kerr black hole we adopt a simple and elegant apparatus described in Stephani *et al.* [12] (Secs. 29.1 and 29.5) to obtain twisting Petrov D vacuum solutions of Einstein's equations. This procedure follows Kerr in his original derivation of the Kerr geometry [1]. The metric is expressed as

$$ds^2 = 2\omega^1\omega^2 - 2\omega^3\omega^4 \tag{1}$$

where the 1-forms ω^a are given by

$$\omega^1 = \bar{\omega}^2 = -d\xi/\bar{\rho}P, \qquad \omega^3 = du + Ld\xi + \bar{L}d\bar{\xi},$$
$$\omega^4 = dr + Wd\xi + \bar{W}d\bar{\xi} + H\omega^3, \tag{2}$$

in Bondi-Sachs–type coordinates $(u, r, \xi, \bar{\xi})$ [7–9,13], where a bar denotes complex conjugation. The metric functions L, W, ρ, H and P are assumed to be independent of the time coordinate u, namely, $\partial/\partial u$ is a Killing vector of the geometry. P is a real function. Einstein's vacuum equations result in (cf. [12])

$$\rho^{-1} = -(r + i\Sigma), \qquad W = i\partial_\xi\Sigma, \tag{3}$$

$$H = \lambda/2 - \frac{mr}{r^2+\Sigma^2}, \tag{4}$$

$$\lambda = 2P^2\mathrm{Re}(\partial_\xi\partial_{\bar{\xi}}\ln P), \tag{5}$$

$$\lambda\Sigma + P^2\mathrm{Re}(\partial_\xi\partial_{\bar{\xi}}\Sigma) = 0, \tag{6}$$

$$2i\Sigma = P^2(\partial_{\bar{\xi}}L - \partial_\xi\bar{L}), \tag{7}$$

where m is a real constant parameter and $\lambda = \pm 1$ is the curvature of the two-dimensional surface $d\xi d\bar{\xi}/P^2$. Here $\lambda = 1$ is adopted. The r-dependence is isolated in ρ and H so that the remaining functions to be determined—P, Σ and L—are functions of $(\xi, \bar{\xi})$ only. By a coordinate transformation we have set the origin of the affine parameter r in Eqs. (3) and (4) equal to zero [12]. The remaining field equations to be integrated reduce then to Eqs. (5), (6) and (7). Here we will substitute the variables $(\xi, \bar{\xi})$ by (θ, ϕ) via the stereographic transformation

$$\xi = \cot(\theta/2)e^{i\phi}.$$

The real function $P(\xi, \bar{\xi})$ is integrated from Eq. (5) by assuming P with the form

$$P = \frac{K(\theta,\phi)}{\sqrt{2}\sin^2(\theta/2)}. \tag{8}$$

Equation (5) reduces then to

$$1 = KK_{\theta\theta} + KK_\theta\cot\theta - K_\theta^2 + K^2 + \frac{(KK_{\phi\phi} - K_\phi^2)}{\sin^2\theta}. \tag{9}$$

$K(\theta,\phi) = 1$ is a solution of Eq. (9) and corresponds to the original Kerr solution. As we will see in the following the general K-function is the proper and natural tool to introduce the boost in asymptotically flat gravitational fields, preserving the asymptotic boundary conditions at future null infinity, even for radiating fields. The K-function actually belongs to the asymptotic orthochronous inhomogeneous Lorentz group that is isomorphic to conformal transformations of the two-sphere into itself, denoted the Bondi-Metzner-Sachs (BMS) group [7–10,13].

A general solution of Eq. (9) is given by

$$K(\theta,\phi) = a + b\hat{x}.\mathbf{n}, \qquad a^2 - b^2 = 1, \tag{10}$$

where $\hat{x} = (\cos\theta, \sin\theta\cos\phi, \sin\theta\sin\phi)$ is the unit vector along an arbitrary direction $\mathbf{x}$ and $\mathbf{n} = (n_1, n_2, n_3)$ is a constant unit vector satisfying

$$n_1^2 + n_2^2 + n_3^2 = 1. \tag{11}$$

The solution (10) has three independent parameters and defines a general Lorentz boost K contained in the homogeneous Lorentz transformations of the BMS group. The boost parameter γ parametrizes a and b as $(a = \cosh\gamma, b = \sinh\gamma)$, and is associated with the velocity $v = \tanh\gamma$ of the black hole relative to a Lorentz frame at future null infinity. The case of a nonboosted solution (the Kerr solution) would correspond to $b = 0$.

Assuming $\Sigma = \Sigma(\theta, \phi)$ Eq. (6) in the variables (θ, ϕ) has the form

$$\Sigma_{\theta\theta} + \cot\theta\Sigma_\theta + \frac{1}{\sin^2\theta}\Sigma_{\phi\phi} + \frac{2\Sigma}{K^2(\theta,\phi)} = 0, \tag{12}$$

from which the regular solution is derived,

$$\Sigma(\theta,\phi) = \omega\frac{b + a(\hat{x}.\mathbf{n})}{a + b(\hat{x}.\mathbf{n})}, \tag{13}$$

where ω is an arbitrary constant to be identified with the rotation parameter of the solution; the parameters $\mathbf{n} = (n_1, n_2, n_3)$ satisfy Eq. (11). For n_2 and/or n_3 nonzero, the black hole solution will be nonaxisymmetric, namely, $\partial/\partial\phi$ is not a Killing vector of the geometry.

Equation (7) can now be integrated using Eq. (13). Adopting accordingly

$$L(\theta,\phi) = i\mathcal{L}(\theta,\phi)e^{-i\phi}, \tag{14}$$

where $\mathcal{L}(\theta,\phi)$ is real, results in

$$\mathcal{L}_\theta - \mathcal{L}/\sin\theta + (1-\cos\theta)\frac{\Sigma(\theta,\phi)}{K^2(\theta,\phi)} = 0. \tag{15}$$

A general solution of Eq. (15) is given by

$$\mathcal{L}(\theta,\phi) = \left(\frac{1-\cos\theta}{\sin\theta}\right)\left[C_1 - \int\frac{\Sigma(\theta,\phi)}{K^2(\theta,\phi)}\sin\theta d\theta\right], \tag{16}$$

where C_1 is an arbitrary constant associated with the solution of the homogeneous part of Eq. (15). Actually C_1 can be an arbitrary function of ϕ which, however, can be rescaled to a constant in the final form of the metric. Furthermore in order to avoid an apparent singular behavior for a zero boost $b^2 = 0$, as occurring in the axisymmetric Kerr boosted case [11], the choice $C_1 = \omega/2b^2$ is adopted in the remainder of the paper. For the general boost equation (10) the integrals in Eq. (16) are expressed

$$\int\frac{\Sigma(\theta,\phi)}{K^2(\theta,\phi)}\sin\theta d\theta = \omega(I_1 + I_2 + I_3 + I_4), \tag{17}$$

where

$$I_1 = b\int\frac{\sin\theta}{K^3(\theta,\phi)}d\theta, \qquad I_2 = an_1\int\frac{\sin\theta\cos\theta}{K^3(\theta,\phi)}d\theta,$$
$$I_3 + I_4 = a(n_2\cos\phi + n_3\sin\phi)\int\frac{\sin^2\theta}{K^3(\theta,\phi)}d\theta. \tag{18}$$

These integrals furnish (by the use of a symbolic manipulation package such as MAPLE) a closed solution in terms of involved combinations of trigonometric functions, and will not be displayed here for lack of space. In particular, in the axisymmetric case, we obtain consistently

$$\int\frac{\Sigma(\theta,\phi)}{K^2(\theta,\phi)}\sin\theta d\theta = \frac{\omega}{2b^2}\frac{a^2 + 2ab\cos\theta + b^2}{(a + b\cos\theta)^2}. \tag{19}$$

The integrands of the integrals in Eq. (18) allows us to define a Bondi-Sachs *4-momentum aspect* as

$$p^\mu(\theta,\phi) = \frac{mk^\mu}{K^3(\theta,\phi)}, \tag{20}$$

where $k^\mu = (-1, \cos\theta, \sin\theta\cos\phi, \sin\theta\sin\phi)$ defines the generators of the BMS translations in the temporal, and Cartesian directions x, y and z of an asymptotic Lorentz frame at future null infinity, and where $K(\theta,\phi)$ given in Eq. (10) is the generator of Lorentz boosts of the BMS [7–10]. The integration of Eq. (20) in the whole sphere yields the total Bondi-Sachs 4-momentum associated with the solution (27) below,

$$P^\mu = \frac{1}{4\pi}\int_0^{2\pi}d\phi\int_0^\pi p^\mu(\theta,\phi)\sin\theta d\theta, \tag{21}$$

namely, the Bondi-Sachs mass $M_{\rm BS}$ and the Bondi-Sachs momentum $\mathbf{P}_{\rm BS}$,

$$M_{\rm BS} = ma = \frac{m}{\sqrt{(1-v^2)}},$$
$$\mathbf{P}_{\rm BS} = mb\mathbf{n} = \frac{mv}{\sqrt{(1-v^2)}}\mathbf{n}. \tag{22}$$

The evaluation of Eq. (21) leading to the result (22) involved a long and careful computation using the *Mathematica* package.

As we will discuss below the mass and momentum aspects (20) are physical quantities that contribute to the angular momentum of the solution.

From Eq. (14) we obtain

$$L d\xi + \bar{L}\,\bar{\xi} = -2\mathcal{L}(\theta,\phi)\cot\theta/2 d\phi, \tag{23}$$

where $\mathcal{L}(\theta,\phi)$ is given by Eq. (16).

Analogously from Eq. (1), $W = i\partial_{\xi}\Sigma$, it results

$$W(\theta,\phi) = e^{-i\phi}\left[-i\Sigma_{\theta}\sin^2\theta/2 + \frac{\Sigma_{\phi}}{2\cot\theta/2}\right], \tag{24}$$

and we obtain

$$\begin{aligned} W d\xi + \bar{W} d\bar{\xi} &= \left[\Sigma_{\theta}\sin\theta d\phi - \frac{\Sigma_{\phi}}{\sin\theta} d\theta\right] \\ &= \omega\left(\frac{-n_1\sin^2\theta + (n_2\cos\phi + n_3\sin\phi)\sin\theta\cos\theta}{K^2(\theta,\phi)}\right) d\phi + \omega\frac{(n_2\sin\phi - n_3\cos\phi)}{K^2(\theta,\phi)} d\theta. \end{aligned} \tag{25}$$

In order to complete the metric 1-forms (2) we have

$$H = \frac{1}{2} - \frac{mr}{r^2 + \Sigma^2(\theta,\phi)}, \qquad \rho^{-1} = -(r + i\Sigma(\theta,\phi)). \tag{26}$$

The metric (1) finally results in

$$\begin{aligned} ds^2 = &\frac{r^2 + \Sigma^2(\theta,\phi)}{K^2(\theta,\phi)}(d\theta^2 + \sin^2\theta d\phi^2) - 2(du - 2\mathcal{L}(\theta,\phi)\cot\theta/2 d\phi) \\ &\times\left[dr + \omega\frac{-n_1\sin^2\theta + (n_2\cos\phi + n_3\sin\phi)\sin\theta\cos\theta}{K^2(\theta,\phi)} d\phi + \omega\frac{n_2\sin\phi - n_3\cos\phi}{K^2(\theta,\phi)} d\theta\right] \\ &- (du - 2\mathcal{L}(\theta,\phi)\cot\theta/2 d\phi)^2 \times \frac{r^2 - 2mr + \Sigma^2(\theta,\phi)}{r^2 + \Sigma^2(\theta,\phi)}. \end{aligned} \tag{27}$$

where $K(\theta,\phi)$ and $\Sigma(\theta,\phi)$ are given in Eqs. (10) and (13), respectively, and $\mathcal{L}(\theta,\phi)$ in Eq. (16). The metric describes a boosted Kerr black hole along an arbitrary direction relative to an asymptotic Lorentz frame at future null infinity. The direction of the boost is defined by the Euler parameters (n_1, n_2, n_3), cf. (10), of the Lorentz boosts of the BMS group [7].

For $n_2 = 0 = n_3$ and $b = 0$ the metric (27) is the original Kerr metric in retarded Bondi-Sachs–type coordinates.[1] For $\omega = 0$ it represents a boosted Schwarzschild black hole along the direction determined by (n_1, n_2, n_3).

By isolating the mass dependent term in the above geometry we obtain

$$ds^2 = ds_M^2 + \frac{2mr}{r^2 + \Sigma^2(\theta,\phi)}(l_{\alpha}dx^{\alpha})^2, \tag{28}$$

where $l_{\alpha} = (1, 0, 0, -2\mathcal{L}(\theta,\phi)\cot\theta/2)$ is a null vector with respect to both metrics ds^2 and ds_M^2, namely, $l_{\alpha}l^{\alpha} = 0$. In verifying these results we used

$$\begin{aligned} g^{uu} &= \frac{4K^2(\theta,\phi)\mathcal{L}^2(\theta,\phi)}{(\cos\theta - 1)^2(r^2 + \Sigma^2(\theta,\phi))}, \\ g^{u\phi} &= -\frac{2K^2(\theta,\phi)\mathcal{L}(\theta,\phi)}{(\cos\theta - 1)\sin\theta(r^2 + \Sigma^2(\theta,\phi))}, \\ g^{\phi\phi} &= \frac{4K^2(\theta,\phi)}{\sin^2\theta(r^2 + \Sigma^2(\theta,\phi))}. \end{aligned}$$

The metric ds_M^2 does not involve the mass and has the associated Riemann tensor equal to zero, as can be tested carefully, being the metric $g_{(M)\alpha\beta}$ of a flat space, so that Eq. (27) assumes the Kerr-Schild form

$$g_{\alpha\beta} = g_{(M)\alpha\beta} + \frac{2mr}{r^2 + \Sigma^2(\theta,\phi)} l_{\alpha}l_{\beta}.$$

[1]We note that these coordinates correspond actually to the standard Kerr-Schild or Eddington-Finkelstein coordinates used largely in the literature of Kerr spacetimes.

As we are in the realm of Kerr metrics it is straightforward to see that in the axisymmetric case, namely, when $n_2 = 0 = n_3$, the metric (27) reduces either to the axial Kerr boosted metric or to the Kerr metric, whether $b \neq 0$ or $b = 0$ respectively, the metrics having the Killing vectors $\partial/\partial u$ and $\partial/\partial \phi$.

Expanding (27) in the axisymmetric case for large r and in the limit of slow rotation parameter $\omega \ll m$, we obtain

$$ds^2 \simeq -\left(1 - \frac{2m}{r}\right) du^2 - 2dudr + \frac{r^2(d\theta^2 + \sin^2\theta d\phi^2)}{K^2(\theta)}, \\ + \frac{4m\omega}{rK^2(\theta)} \sin^2\theta du d\phi, \tag{29}$$

where $K(\theta) = (a + b\cos\theta)$. This linearized version represents a boosted mass monopole plus the Lense-Thirring rotating term with angular momentum $m\omega$ [14–16]. Therefore in the axisymmetric case the metric (27) can then be interpreted as a boosted Kerr black hole rotating about the z axis (the axis defining the angle ϕ) with angular momentum $m\omega$. The boost is along the axis of rotation, relative to an asymptotic Lorentz frame at future null infinity.

Now for the general boosted case an analogous expansion results in

$$ds^2 \simeq -\left(1 - \frac{2m}{r}\right) du^2 - 2dudr + \frac{r^2(d\theta^2 + \sin^2\theta d\phi^2)}{K^2(\theta,\phi)} \\ - \frac{4m}{r}\mathcal{L}(\theta,\phi)\cot\theta/2 du d\phi. \tag{30}$$

By comparing Eqs. (29) and (30) we observe that a difference appears in the Lense-Thirring rotation term. This actually results from the fact that—besides the mass aspect—the rotation term of Eq. (29) contains just the *3-momentum aspect* component p^1 of the geometry, while in Eq. (30) the complete 3-momentum aspect (p^1, p^2, p^3) is present. In this sense we have in Eq. (30) a genuine natural extension of the Lense-Thirring rotation term. The vanishing of the components p^2 and p^3 of the 3-momentum aspects (20), by taking $n_2 = 0 = n_3$, restores the axisymmetry of the boosted black hole configuration. We remark that the presence of a momentum aspect that adds to the mass aspect in Eq. (17) is mandatory since we cannot make all the Euler parameters zero due to the relation $n_1^2 + n_2^2 + n_3^2 = 1$. In all cases the angular momentum is proportional to $m\omega$ about the axis defining the coordinate ϕ.

We note that the $1/K^2$-factor multiplying the two-sphere line element in Eqs. (29) and (30) is actually a conformal transformation of the unit two-sphere into itself which is isomorphic to a Lorentz boost of the BMS group [10,13]. The z axis about which the black hole rotates does not coincide with the boost axis except in the axial case $n_2 = 0 = n_3$ [11]. A further detailed examination of the rotation term $du d\phi$ of the Kerr boosted geometry (27) will be given in the following section, where the angular momentum of the event horizon $r = r_+$ is analyzed.

Finally for illustration and comparison with the above results we present the slow rotation limit of a nonboosted nonaxisymmetric Kerr black hole [cf. (27)] that reads

$$ds^2 \simeq -\left(1 - \frac{2m}{r}\right) du^2 - 2dudr + r^2(d\theta^2 + \sin^2\theta d\phi^2) \\ + \frac{4m\omega}{r}(n_1\sin^2\theta + (n_2\cos\phi + n_3\sin\phi) \\ \times(\theta - \sin\theta\cos\theta))du d\phi. \tag{31}$$

The angular momentum at the equator in this case results in $\Omega(\phi) = m\omega(n_1 + \pi(n_2\cos\phi + n_3\sin\phi)/2)$.

III. PROPERTIES OF THE SOLUTION: THE ERGOSPHERE AND HORIZONS

A direct examination of Eq. (27) shows that $\partial/\partial u$ is a Killing vector of the geometry and defines its stationary character. The general boosted Kerr geometry also presents an ergosphere, defined by the limit surface for static observers, namely, the locus where the Killing vector $\partial/\partial u$ becomes null [16], and by the event horizon to be discussed below. In the coordinate system of Eq. (27) the equation of the limit surface $g_{uu} = 0$ results in

$$r^2 - 2mr + \Sigma^2(\theta,\phi) = 0, \tag{32}$$

or

$$r_{\rm stat}(\theta,\phi) = m + \sqrt{m^2 - \Sigma^2(\theta,\phi)}. \tag{33}$$

The horizons are the surfaces defined by

$$g^{rr} = \frac{1}{r^2 + \Sigma^2(\theta,\phi)}\left[r^2 - 2mr + \omega^2\frac{\Delta(\theta,\phi)}{K^2(\theta,\phi)}\right] = 0, \tag{34}$$

where

$$\Delta(\theta,\phi) = (b + a\hat{x}.\mathbf{n})^2 + \Delta_1(\theta,\phi),$$

and

$$\Delta_1(\theta,\phi) = n_1^2\sin^2\theta + n_2^2(\cos^2\phi\cos^2\theta + \sin^2\phi) \\ + n_3^2(\cos^2\phi\sin^2\theta + \cos^2\theta) \\ - 2n_1n_2(\sin\theta\cos\theta\cos\phi) \\ - 2n_1n_3(\sin\theta\cos\theta\sin\phi) \\ - 2n_2n_3(\sin^2\theta\sin\phi\cos\phi). \tag{35}$$

Since $(n_1^2 + n_2^2 + n_2^2) = 1$ and $(a^2 - b^2) = 1$ for a general boost, cf. (10), it follows after some algebra that

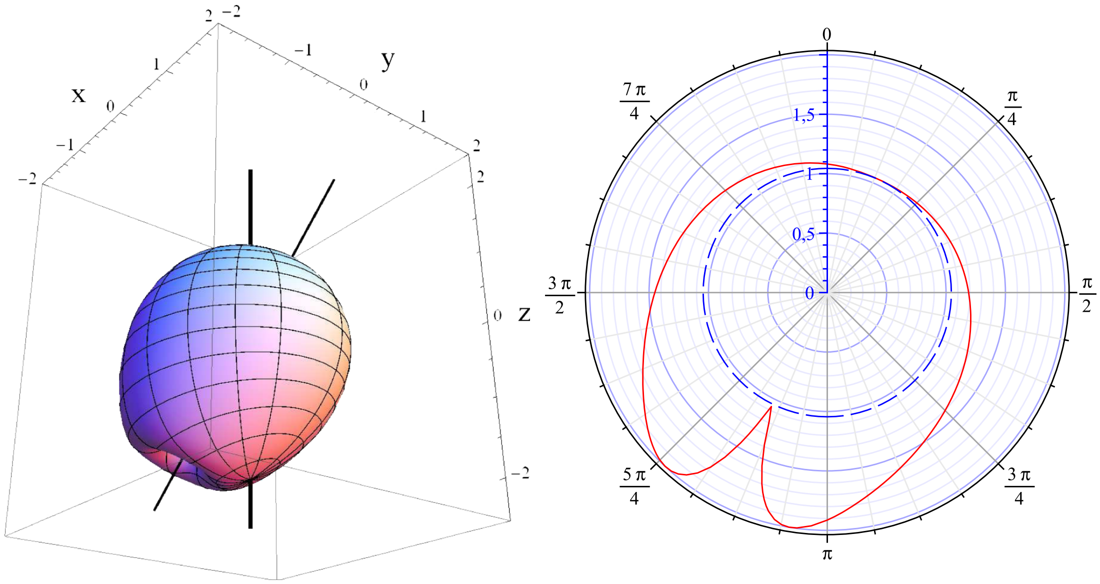

FIG. 1. Plots of the ergosphere for a boosted Kerr black hole, with $m = 1$, $\omega = 0.999$ and the boost direction taken as $n_1 = 0.9$, $n_2 = 0.3$, $n_3 \simeq 0.316227766$. The boost parameters b and a correspond to the velocity of the black hole $v/c \simeq 0.956532$. (Left panel) A three-dimensional view of the ergosphere static limit where the thin black axis corresponds to the direction (n_1, n_2, n_3) of the boost while the thick black axis is the axis of rotation (the z axis) of the black hole. (Right panel) A section of the ergosphere static limit by the plane $\phi = \pi/3.931$ (red continuous line) shown in the plane θ. The boost axis shown in the left figure is defined by the two points $\theta \simeq 25.84°$ and $\theta \simeq 25.84° \pm \pi$ where the ergosphere contacts the two-dimensional event horizon $r_+ \simeq 1.044710$ (dashed blue line).

$\Delta(\theta, \phi)/K^2(\theta, \phi) = 1$, so that Eq. (34) reduces to the simple form

$$r^2 - 2mr + \omega^2 = 0,$$

with roots

$$r_\pm = m \pm \sqrt{m^2 - \omega^2}. \tag{36}$$

We can see that the event horizon r_+ and the Cauchy horizon r_- do not alter by the effect of the boost.

The region between the surfaces $r_{\rm stat}$ and r_+ is the ergosphere where the Penrose process [17,18] takes place. The ergosphere is deformed along the direction $\mathbf{n} = (n_1, n_2, n_3)$ of the boost, as illustrated in Fig. 1 (left panel) for a Kerr black hole with mass $m = 1$ and rotation parameter $\omega = 0.999$, in geometrical units. The boost parameter adopted to construct the figure was $b = 3.28$, corresponding to the boost velocity of the black hole $v/c = \tanh\gamma \simeq 0.956532$, relative to a Lorentz frame at null infinity. The ergosphere static limit surface contacts the event horizon r_+ in just two points. In the configuration of Fig. 1 (right panel) these points correspond to $\phi = \pi/3.931$, with $\theta \simeq 25.84°$ and $\theta \simeq 25.84° \pm \pi$.

Both horizons r_+ and r_- constitute three-dimensional manifolds with the topology of S^3, although the associated geometry is not spherical. This property—already known for the case of the original Kerr black hole spacetime [19,20]—holds also for the boosted extensions of the Kerr manifold. For the sake of simplicity and space we consider the case of the event horizon $r = r_+$ only, and the restriction to the section $\theta = \pi/2$ of the geometry (27). The case of the Cauchy horizon r_- has a similar analysis and results. We obtain

$$\begin{aligned} ds^2| &= \Omega(\phi) du d\phi - \left(\frac{\Sigma^2(\pi/2,\phi) - \omega^2}{r_+^2 + \Sigma^2(\pi/2,\phi)}\right) du^2 \\ &\quad + \left(\frac{r_+^2 + \Sigma^2(\pi/2,\phi) - 4\mathcal{L}(\pi/2,\phi)\omega n_1}{K^2(\pi/2,\phi)} \right. \\ &\quad \left. - 4\mathcal{L}(\pi/2,\phi)\left[\frac{\Sigma^2(\pi/2,\phi) - \omega^2}{r_+^2 + \Sigma^2(\pi/2,\phi)}\right]\right) d\phi^2, \end{aligned} \tag{37}$$

where

$$\begin{aligned} \Omega(\phi) &= 2\omega\left(\frac{n_1}{K^2(\pi/2,\phi)} + \frac{2\mathcal{L}(\pi/2,\phi)(\Sigma^2(\pi/2,\phi) - \omega^2)}{\omega(r_+^2 + \Sigma^2(\pi/2,\phi))}\right), \\ \Sigma^2(\pi/2,\phi) - \omega^2 &= \omega^2 \frac{(n_2\cos\phi + n_3\sin\phi)^2 - 1}{K^2(\pi/2,\phi)}, \\ K(\pi/2,\phi) &= a + b(n_2\cos\phi + n_3\sin\phi). \end{aligned} \tag{38}$$

The term $\Omega(\phi)$ of the restricted geometry (37) corresponds to a rotation about the z axis. The associated angular momentum is not conserved since $\partial/\partial\phi$ is not a Killing vector of the black hole geometry. Furthermore from Fig. 1 we also can see that the angle between the boost axis, defined by the Euler parameters (n_1, n_2, n_3), and the rotation axis z is $\theta_0 = \arccos(n_1)$.

If we consider the axisymmetric limit of Eq. (27), the rotational term of the event horizon $r = r_+$ at the equatorial plane $\theta = \pi/2$ reduces to

$$\Omega = \omega \frac{4mr_+}{(a^2 r_+^2 + \omega^2 b^2)}. \tag{39}$$

Finally the geometry of the event horizon at the section $du = 0$ results in

$$ds^2| = \frac{r_+^2 + \Sigma^2(\theta)}{(a + b\cos\theta)^2}(d\theta^2 + \sin^2\theta d\phi^2) + \frac{\omega^2 \sin^4\theta}{(a + b\cos\theta)^4}\left(\frac{r_+^2 + \Sigma^2(\theta) + 2mr_+}{r_+^2 + \Sigma^2(\theta)}\right)d\phi^2, \tag{40}$$

which is topologically, but not geometrically, a two-sphere. For the general boosted Kerr black hole this property can be checked numerically.

IV. THE SINGULARITY

By a careful examination of the curvature invariants of Eq. (27) we can see that the metric and the curvature are truly singular at

$$r^2 + \Sigma^2(\theta, \phi) = 0, \tag{41}$$

namely, at

$$r = 0, \qquad \Sigma(\theta, \phi) = 0. \tag{42}$$

The singularity is then contained in the two-dimensional surface defined by

$$(n_1 \cos\theta + n_2 \sin\theta\cos\phi + n_3 \sin\theta\sin\phi) = -b/a, \tag{43}$$

at $r = 0$. Specifically the singular points correspond to closed curves which are the intersection of the two-dimensional surface $\mathcal{H}(\theta, \phi)$ with the two-sphere $\mathcal{S}(\theta, \phi) = b/a$ with center at the origin,

$$\mathcal{H}(\theta,\phi) = (n_1 \cos\theta + n_2 \sin\theta\cos\phi + n_3 \sin\theta\sin\phi), \tag{44}$$

$$\mathcal{S}(\theta, \phi) = -b/a, \quad \text{for all} \quad (\theta, \phi). \tag{45}$$

For increasing values of $|b|$—as the radius of the (red) sphere $\mathcal{S}(\theta, \phi)$ about the origin increases—the radius of the singularity lines initially increases and then decreases. In the limits $b = 0$ and $b \to \infty$ (that is, when $b/a = v/c \to 1$) the closed curves reduce to a point. This is illustrated in Fig. 2 for of $b = -0.15$, -0.45 and -1.8.

For the axisymmetric boosted case ($n_1 = 1$ and $n_2 = 0 = n_3$) the closed curves corresponding to the singularity of the black hole are circles on the planes $z =$ const [namely, $\theta_S = \arccos(-b/a)$], with $0 < |b| < \infty$, as illustrated in Fig. 3 for $b = -0.1$, $b = -0.45$ and $b = -1.2$. Analogous to the general boosted case, for $b \to \pm\infty$ the singularity circle reduces to a point at the north/south poles ($\theta = 0, \pi$); for $b = 0$ (the Kerr black hole) the circle reduces to a point on the equatorial plane.

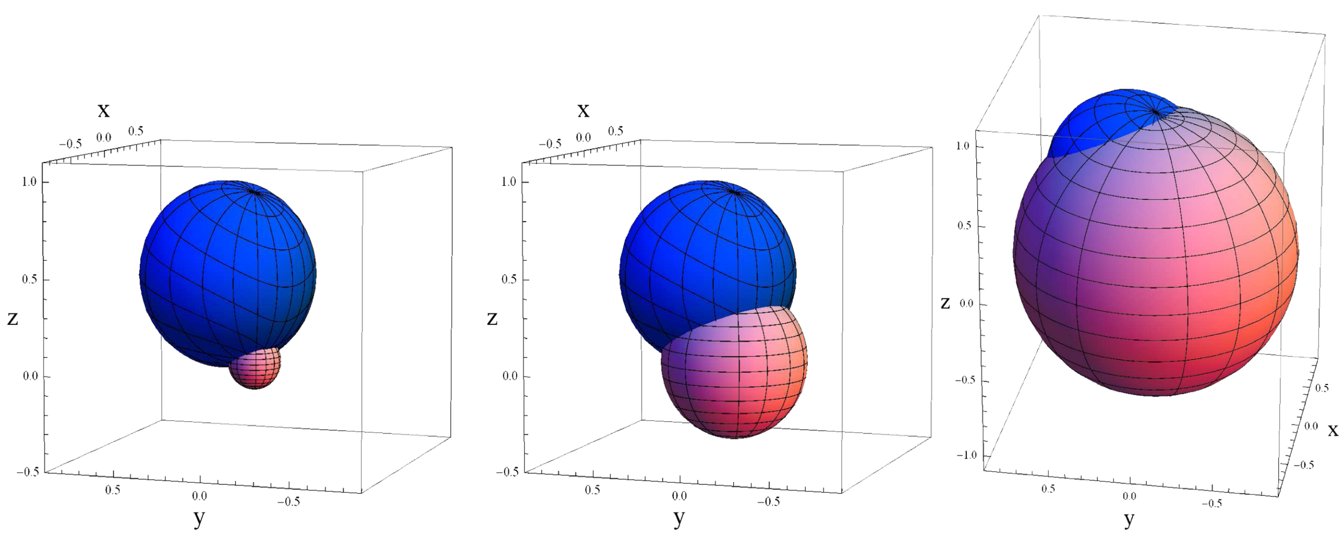

FIG. 2. Plots of the intersections of the surface $\mathcal{H}(\theta, \phi) = (n_1 \cos\theta + n_2 \sin\theta\cos\phi + n_3 \sin\theta\sin\phi)$ (blue) with the sphere $\mathcal{S}(\theta, \phi)$ about the origin with radius $-(b/a)$ (red). The intersection defines a closed line of singularities; for increasing values of $|b|$ these closed curves increase and then decrease as the radius of the spherical surface (red) about the origin increases. The figures correspond to the three values of $b = -0.15$, $b = -0.45$ and $b = -1.8$ (from left to right), with fixed parameters ($n_1 = 0.9, n_2 = 0.2, n_3 = \sqrt{1 - n_1^2 - n_2^2}$). For $b = 0$ and $b \to \pm\infty$ the circles reduce to a point. The closed singularity curves are contained in planes orthogonal to the direction of the boost (n_1, n_2, n_3).

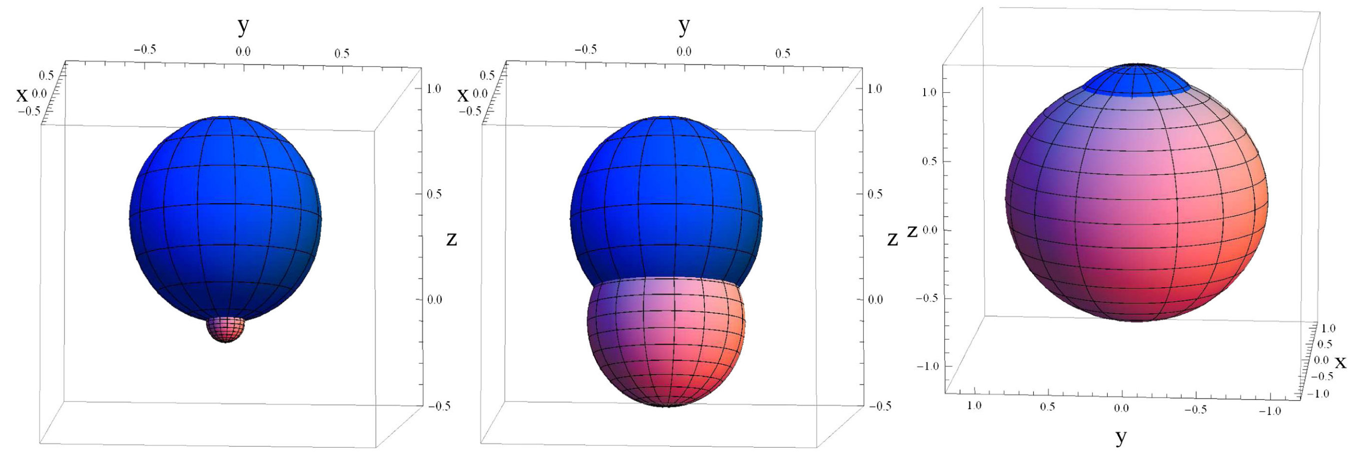

FIG. 3. Plot of the intersection of the surface $\mathcal{H}(\theta,\phi)$ (blue) and the sphere $\mathcal{S}(\theta,\phi)$ (red) for the axial boosted case, with $n_1 = 1$, $n_2 = 0 = n_3$ and $b = -0.1$, $b = -0.45$ and $b = -1.2$ (from left to right). The intersections are circles of singularity on the $z = \text{const}$ (or $\theta = \text{const}$) planes, as should be expected in the axial configuration. For $b = 0$ and $|b| \to \infty$ the circles reduce to a point respectively at the equatorial plane $\theta = \pi/2$ and at the poles $\theta = 0, \pi$.

The point singularities occurring at the equatorial plane and at the north/south poles (corresponding respectively to $b = 0$ and $b \to \pm\infty$) can be developed by using the flat metric ds^2_M of the Kerr-Schild form (28). A straightforward calculation yields that in the axial case $\mathcal{L}(\theta,\phi)_S = -\omega(a+b)/2$ so that the background geometry ds^2_M in Eq. (28) assumes the form

$$ds^2_M|_S = -du^2 + \omega^2 d\phi^2,$$

independent of b, so that in terms of the Minkowski metric ds^2_M the curvature singularity at $\theta = \pi/2$ and $\theta = 0, \pi$ has the topology of a ring [19]. This pattern is to be maintained for the general boosted case except that the closed singularity curves are obviously no longer on the equatorial plane, being actually contained in planes orthogonal to the direction of the boost determined by (n_1, n_2, n_3).

V. DISCUSSIONS AND CONCLUSIONS

In this paper we have derived a solution of Einstein's vacuum equations (27) corresponding to a general boosted Kerr black hole that describes the most general configuration of a remnant astrophysical black hole present in nature.

Astrophysical processes in which black holes are formed were the object of recent detections by the LIGO Scientific Collaboration and the Virgo Collaboration [21], of the gravitational waves emitted by a binary black hole merger [3–6] with mass ratios in the range 0.53–0.83. The unequal masses of the initial black holes in the observed binaries result that the gravitational waves emitted have a nonzero gravitational wave momentum flux, indicating that the remnant black hole must be a Kerr black hole boosted along the direction of the late time momentum flux, with respect to the asymptotic Lorentz frame at null infinity where such emissions have been detected. The remnant black hole solution has five independent parameters, namely, the mass m, the rotation parameter ω, the boost velocity $v = \tanh\gamma$ and the direction of the boost determined by (n_1, n_2, n_3) satisfying $(n_1)^2 + (n_2)^2 + (n_3)^2 = 1$. These parameters are necessary to the description of a remnant black hole in nature. In the integration of the solution the general $K(\theta,\phi)$-function appears as the appropriate and natural tool to introduce the boost in asymptotically flat gravitational fields, preserving the asymptotic boundary conditions at future null infinity. The additional parameters connected to the boost do not change the Kerr black hole structure, namely, the event and the Cauchy horizons, both having the topology of a three-sphere. The paper extends our previous results obtained in the axisymmetric case [11].

The issue of the rotation of the black hole is examined firstly in the case of large r and the slow rotation limit. We obtain that this linearized version represents a boosted mass monopole plus the Lense-Thirring rotating term with angular momentum proportional to $m\omega$ about the axis defining the angle ϕ. By comparing the axisymmetric and nonaxisymmetric case we observe that the difference in the Lense-Thirring rotation term results basically from the fact that—besides the mass aspect—the rotation term in the axisymmetric case contains just the 3-momentum aspect p^1 of the geometry, while in the nonaxisymmetric case the complete 3-momentum aspect (p^1, p^2, p^3) is present. This clarify the extension of the Lense-Thirring rotation term for the general boosted case. We note that the momentum aspects p^2 and p^3 break the rotational symmetry about the z axis so that the angular momentum varies as the black hole rotates about the z axis; $\partial/\partial\phi$ is obviously not a Killing vector of the metric. In the limit of p^2 and p^3 going continuously to zero (30) tends continuously to (29) as expected.

The static limit surface and the ergosphere are also examined in the case of the general boosted Kerr black hole; as in the axisymmetric case the general boost turns the ergosphere asymmetric in the direction opposite to the boost.

The singularity at $r = 0$, $\Sigma(\theta, \phi) = 0$ corresponds to closed curves contained in two-dimensional planes orthogonal to the direction of the boost determined by (n_1, n_2, n_3). For increasing values of the boost parameter $|b|$ the radius of the singularity lines initially increase and then decreases. In the limits $b = 0$ (that is, when $b/a = v/c = 0$) and $b = \to\infty$ (that is, when $b/a = v/c \to 1$) the closed curves reduce to a point. The point singularities occurring at the equatorial plane and at the north/south poles (corresponding respectively to $v = 0$ and $v \to 1$) can be developed, in the Minkowski background, into curves with the topology of a ring.

Actually the boosted black hole solution can be a natural set for astrophysical processes connected to the asymmetry of the ergosphere and to electromagnetic dynamical effects that may result from the rotating black hole moving at relativistic speeds in a direction not coinciding with the rotation axis. In this setting electromagnetic losses due to translational and rotational motion of the black hole are expected to occur. These effects may correspond to the electromagnetic counterpart of the gravitational wave emission by the black hole having possibly the same order of magnitude, and can eventually turn out to be important for the astrophysics of highly energetic bounded sources observed in our actual Universe (as for instance AGN) as we comment below.

We envisage that these processes can have applications in modeling the astrophysics of electromagnetic outflows involving the boost and rotation encompassed in the black hole (27). In fact rotating black holes in electrovacuum or in a tenuous plasma can produce strong electromagnetic signals similar to the magnetospheres of rotating pulsars as in the Blandford-Znajek processes [22–24]. Another aspect has to do with the motion of the black hole at relativistic speeds in such an environment. The electromagnetic fields can either be of external origin or due to the motions of the constituents of the plasma itself. Electric currents flowing in the plasma may induce a time dependent magnetic field $\mathbf{B}$ in a plane orthogonal to the rotation axis. Furthermore, since the rotation axis makes an angle $\theta = \arccos(n_1)$ with the boost direction, a further nonzero electric field component proportional to $(\mathbf{v} \wedge \mathbf{B})$ will be present. This makes possible the appearance of electromagnetic flows that may appear as an electromagnetic counterpart of late time emissions in the merger of black holes [25–28]. We recall that this boost is inherited from the net momentum flux of the gravitational waves emitted in the collision and merger of two nonequal mass black holes that generated the remnant.

Finally we argue that the application of such mechanisms as engines of relativistic electromagnetic jets from quasars, pulsars and AGN could be properly considered and implemented in the neighborhood of the general boosted Kerr black hole (27). We are presently examining numerically solutions of Maxwell equations in the background of the black hole (27) taking into account a tenuous plasma as source, with a view to the evaluation of the electromagnetic power emitted in these configurations (cf. also Abdujabbarov *et al.* [29] for the axisymmetric case [11]). Recently Benavides-Gallego *et al.* [30] studied weak gravitational lensing around a boosted Kerr black hole [11] in the presence of plasma.

ACKNOWLEDGMENTS

The author acknowledges the partial financial support of CNPq/MCTI-Brazil, through Research Grant No. 308728/2017-3. The author is also grateful to an anonymous referee for criticisms and comments that contributed to a substantial improvement of the paper.

[1] R. P. Kerr, Phys. Rev. Lett. **11**, 237 (1963).
[2] K. Schwarzschild, Berliner Sitzungbesichte Akad. Wiss. Berlin (Phys. Math. Klasse) 189–196 (1916).
[3] B. P. Abbott *et al.* (LIGO and Virgo Collaborations), Phys. Rev. Lett. **116**, 061102 (2016).
[4] B. P. Abbott *et al.* (LIGO and Virgo Collaborations), Phys. Rev. Lett. **116**, 241103 (2016).
[5] B. P. Abbott *et al.* (LIGO and Virgo Collaborations), Phys. Rev. Lett. **119**, 141101 (2017).
[6] B. P. Abbott *et al.* (LIGO and Virgo Collaborations), Phys. Rev. Lett. **118**, 221101 (2017).
[7] H. Bondi, M. G. J. van der Berg, and A. W. K. Metzner, Proc. R. Soc. A **269**, 21 (1962).
[8] R. K. Sachs, Proc. R. Soc. A **270**, 103 (1962).
[9] R. K. Sachs, J. Math. Phys. (N.Y.) **3**, 908 (1962).
[10] R. K. Sachs, Phys. Rev. **128**, 2851 (1962).
[11] I. D. Soares, Gen. Relativ. Gravit. **49**, 77 (2017).
[12] H. Stephani, D. Kramer, M. A. H. MacCallum, C. Hoenselaers, and E. Herlt, *Exact Solutions of Einstein's Field Equations*, 2nd ed. (Cambridge University Press, Cambridge, England, 2003).
[13] E. T. Newman and R. Penrose, J. Math. Phys. (N.Y.) **7**, 863 (1966).
[14] H. Thirring and J. Lense, Phys. Z. **19**, 156 (1918).
[15] E. T. Newman and A. I. Janis, J. Math. Phys. (N.Y.) **6**, 915 (1965).

[16] E. Poisson, *A Relativist's Toolkit: The Mathematics of Black-Hole Mechanics* (Cambridge University Press, Cambridge, England, 2004).

[17] R. Penrose, Riv. Nuovo Cimento Soc. Ital. Fis. **1**, 252 (1969).

[18] C. W. Misner, K. S. Thorne, and J. A. Wheeler, *Gravitation* (W.H. Freeman and Company, San Francisco, 1970).

[19] M. Visser, arXiv:0706.0622v3.

[20] L. Smarr, Phys. Rev. D **7**, 289 (1973).

[21] B. P. Abbott *et al.* (LIGO Scientific Collaboration), Rep. Prog. Phys. **72**, 076901 (2009); G. M. Harry (LIGO Scientific Collaboration), Classical Quantum Gravity **27**, 084006 (2010).

[22] R. D. Blanford and R. Znajek, Mon. Not. R. Astron. Soc. **179**, 433 (1977).

[23] S. Koide, K. Shibata, T. Kudoh, and D. L. Maier, Science **295**, 1688 (2002); S. Koide and T. Baba, Astrophys. J. **792**, 88 (2014).

[24] P. Moesta, C. Palenzuela, L. Rezzolla, L. Lehner, S. Yoshida, and D. Pollney, Phys. Rev. D **81**, 064017 (2010).

[25] M. Lyutikov, Phys. Rev. D **83**, 064001 (2011).

[26] P. Moesta, D. Alic, L. Rezzolla, O. Zanotti, and C. Palenzuela, Astrophys. J. Lett. **749**, L32 (2012).

[27] D. Alic, P. Moesta, L. Rezzolla, O. Zanotti, and J. L. Jaramillo, Astrophys. J. **754**, 36 (2012).

[28] V. S. Morozova, L. Rezzolla, and B. J. Ahmedov, Phys. Rev. D **89**, 104030 (2014).

[29] A. Abdujabbarov, N. Dadhich, and B. Ahmedov, arXiv: 1810.08066.

[30] C. A. Benavides-Gallego, A. A. Abdujabbarov, and C. Bambi, Eur. Phys. J. C **78**, 694 (2018).